Molecular and Ultrastructural Studies of a Fibrillar Collagen from Octocoral (Cnidaria)

Joseph P.R.O. Orgel[1,2,3,*], Ido Sella[4], Rama S. Madhurapantula[2], Olga Antipova[2,3], Yael Mandelberg[4], Yoel Kashman[5], Dafna Benayahu[6], and Yehuda Benayahu[4,*]

[1]Departments of Biology, Physics and Biomedical Engineering, Illinois Institute of Technology
[2]Pritzker Institute of Biomedical Science and Engineering, Illinois Institute of Technology 3440 S. Dearborn Ave, Chicago, IL 60616, USA
[3]BioCAT, Advanced Photon Source, Argonne National Laboratory, IL
[4]School of Zoology, George S. Wise Faculty of Life Sciences, Tel Aviv University, Ramat Aviv, Tel Aviv 69978, Israel
[5]School of Chemistry, Faculty of Exact Sciences, Tel Aviv University, Ramat Aviv, Tel Aviv 69978, Israel
[6]Department of Cell and Developmental Biology, Sackler School of Medicine, Tel Aviv University, Tel Aviv 69978, Israel

*Corresponding Authors: Joseph PRO Orgel: orgel@iit.edu, Yehuda Benayahu: YehudaB@tauex.tau.ac.il

Keywords: Fibrillar collagen | X-ray diffraction | microscopy | Cnidaria | d-period | Red Sea

Summary statement

We report here, structural and biochemical features of a previously unknown fibrillar collagen from an octocoral and its similarities to mammalian type I and II collagens.

Abstract

We report here the biochemical, molecular and ultrastructural features of a unique organization of fibrillar collagen extracted from the octocoral *Sarcophyton ehrenbergi*. Collagen, the most abundant protein in the animal kingdom, is often defined as a structural component of extra-cellular matrices in metazoans. In the present study, collagen fibers were extracted from the mesenteries of *S. ehrenbergi* polyps. These fibers are organized as filaments and further compacted as coiled fibers. The fibers are uniquely long, reaching an unprecedented length of tens of centimeters. The diameter of these fibers is 9 ±0.37 μm.The amino acid content of these fibers was identified using chromatography and revealed close similarity in content to mammalian type I and II collagens. The ultrastructural organization of the fibers was characterized by means of high resolution microscopy and X-ray diffraction. The fibers are composed of fibrils and fibril bundles in the range of 15 to 35 nm. These data indicate a fibrillar collagen possessing structural aspects of both types I and II, a highly interesting and newly described form of fibrillar collagen organization.

1 Introduction

Collagens are a heterogeneous family of extracellular matrix proteins and are abundant in a plethora of species, ranging from bacteria, fungi, invertebrates and vertebrates (Exposito et al., 2010).The collagen family is divided into fibrillar and non-fibrillar categories based on packing and ultrastructure. Fibrillar type I collagen is the single most abundant protein (by mass) in animals. A characteristic feature of the fibrillar collagen molecule is its triple-helical domain, where three collagen polypeptide chains are wound around one another to form a rope-like super-helix. The polypeptide chains predominantly contain a repeating Glycine(G)-X-Y peptide sequence where the X and Y positions are usually occupied by Proline (P) and Hydroxyproline (O). This organization is important for the proper formation of the collagen helix. The Glycine - Proline(P) - Hydroxyproline(O) sequence is prominent in the C-terminal region, where several successive GPO repeats appear to drive triple-helix polymerization (Swatschek et al., 2002).

Fibrillar collagens are hierarchically organized with a higher order in axial packing to form long fibers. Type I collagen molecules are packed into a quasi-hexagonal array featuring micro-fibrils of 4-5 nm in diameter (Orgel et al., 2006). The fibrils are composed of micro-fibrils made of five D-staggered neighboring collagen molecules, where D is normally ~ 67 nm, forming the Hodge-Petruska scheme of axial organization. This consists of five molecular segments within an overlap region and four in the gap which is easily recognized by transmission electron microscopy (TEM) (Petruska and Hodge, 1964).

Journal of Experimental Biology • Advance article

The occurrence of fibrillar (such as type I) and the basement membrane (type IV) collagens has been described in the earliest branching multicellular animals, namely Porifera and Cnidaria (Exposito et al., 2008).The body wall of cnidarians is organized from an epithelial bilayer with an intervening acellular component, featuring mainly mesoglea that contain tiny, dispersed, collagen fibers (Fautin and Mariscal, 1991). These fibers are markedly different in appearance, from cord-like collagen fibers (CLCF). Collagen fibers may appear histologically similar in the mesoglea of different Cnidarian species, but can exhibit biochemical features of either fibrillar or basement membrane matrices, creating a structure of scattered and/or organized short fibers that are microscopic in size (Fabricius and Alderslade, 2001).

Current insights into the fibrillar packing of collagen found in the mesoglea of cnidarians come mainly from studies on Hydra and jellyfish. However, analogous data is very limited for collagen from *Sarcophyton* species. A search on the taxonomy browser on NCBI (http://www.ncbi.nlm.nih.gov/) revealed that even with the widely expanding genomic knowledge, only a few genes/proteins were identified for *Sarcophyton* species (Octocorallia, Alcyonacea), none of which are related to the collagen family. Mandelberg et al., 2016 describes microanatomical and biochemical properties of collagen fibers extracted from *S. auritum* colonies. Other works on collagen isolated from the *Sacrophyton* species have been used in making composites for soft-tissue biomimetics (Sharabi et al., 2015, 2016).

The hallmark function of collagen fibers embedded in the mesoglea of these cnidarians is to provide structural support. Long fibers are easily visible when a shallow perpendicular surface-rupture of the coral-colony is conducted. The fibrillar packing of collagen fibers in the mesentery of *S. ehrenbergi* is largely similar to that found in *S. auritum*, at a microscopic level. The anatomical localization of these fibers is also similar between these species (Mandelberg et al., 2016). However, the molecular and the ultrastructural organization of these CLCF differs markedly from the tiny collagen fibers embedded within the cnidarian mesoglea, albeit their biochemical similarities (Exposito et al., 2010).

In the current study, we elaborate on the unique molecular and ultrastructural organization of CLCF isolated from the reef dwelling octocoral *Sarcophyton ehrenbergi*. *S. ehrenbergi* colonies grow in well illuminated parts of the reef into mushroom shaped colonies (Fig. 1A). The gastrovascular cavity of these cnidarians consists of cord-like fibers stretching out from the mesenteries, which are visible to naked eye (Fig.1B). These fibers can be observed upon performing a shallow incision of the polyp surface, perpendicular to the long axis. The length of the pulled fibers may reach a few tens of centimeters and thus differ from the common thinner and much shorter fibers found in the mesoglea. The ultrastructural analyses presented here are supported by the similarity in amino acid content of these fibers to other fibrillar collagens, as determined by high-performance liquid chromatography (HPLC). This further validates the use of molecular structure and packing information previously collected for type I and II collagen (structure factors and phases) to determine the packing features of this plausibly novel class of collagen from *S. ehrenbergi*.

The fibers isolated from *S. ehrenbergi* were stained with Masson's Trichrome, a classic histological stain for fibrillar collagen. Transmission Electron Microscopy (TEM) was also performed on these fibers, which demonstrated the typical pattern of D-periodic striation and parallel fibers arrangement as known for mammalian fibrillar collagen type I. Biochemical analyses show that these fibers indeed belong to the fibrillar collagen subfamily.

Molecular packing features of these fibers were obtained with the use of X-ray fiber diffraction (XRD). These data suggest that aspects of vertebrate type I and II collagen packing can be observed in these CLCF. The unique XRD patterns and the 1-D electron density profiles constructed from them suggest that these cord-like fibers are formed from a fibrillar collagen similar to that seen in vertebrates. We present here, the first data to demonstrate molecular packing of these long CLCF obtained from *S. ehrenbergi* that has features of fibrillar packing observed in type I and II collagen, while not being clearly, one type of the other as judged from the structural data presented here (Sella, 2012).

2 Materials and Methods

Methods for sample collection, histology, microscopy and amino acid analysis were reported to analyze fibers obtained from *S. auritum* in Mandelberg et al. (2016) (Mandelberg et al., 2016). These methods can be applied for similar analysis on fibers extracted from *S. ehrenbergi*, as these organisms belong to the same genus.

2.1 Sample collection

Fragments of *S. ehrenbergi* (3-4 cm^3) were removed from the polyp bearing part of the colony as previously described (Fabricius and Alderslade, 2001). Samples were collected from the reefs of Dahalak Archipelago (southern Red Sea) and Eilat (Gulf of Aqaba, northern Red sea) at a depth of 3-5 m. They were individually placed, underwater, in zip-lock bags and immediately brought to the laboratory for further processing.

2.2 Histological evaluation of gastrovascular cavity

Samples were removed from colonies that had been previously preserved in 4% glutaraldehyde in seawater. These samples were decalcified, twice, by incubating them in a mixture of equal volumes of formic acid (50%) and sodium citrate (15%) for 20 minutes, and then transferred back to 4% glutaraldehyde. They were then rinsed with distilled water, and embedded in 2% agarose (50°C), or in high melting point paraffin. Following solidification, rectangular pieces, closely fitting around each sample, were cut out and dehydrated using a graded series of ethanol. The samples were then embedded in paraffin. 5-8 μm crosssections were prepared using MIR microtome (Thermo Fisher Scientific, Waltham, MA). Sections were stained with Manson's Trichrome which stains collagen (Ross and Pawlina, 2006).

2.3 Light microscopy on isolated fibers

Isolated fibers were fixed in 4% formaldehyde in seawater, rinsed with distilled water, and preserved in 70% ethanol. The subsamples were placed in paraffin (56°C) and 6-7μm cross-sections were obtained using a microtome (M1R, SHANDON). The sections were stained with Masson's Trichrome (Ross and Pawlina, 2006). Fibrillar collagen is stained with a turquoise color with this histology stain. These stained sections were examined under a Optiphot microscope (Nikon, Japan) (Mandelberg et al., 2016).

2.4 Protein and Amino acid analysis

In order to characterize the protein that composes the fibers, amino acid analysis was preformed at the Department of Chemical Research Support, Weizmann Institute of Science. The method described in Bütikofer et al., (1991) was employed to determine amino acid composition and free amino acids in protein hydrolysates (Bütikofer et al., 1991).

Briefly, hydrolysates were prepared by treating the crushed fibers with several volumes of tri-sodium citrate di-hydrate for a short time and then diluting this mixture using deionized water. Internal standards were then added to the mixture and was then incubated at 40°C with occasional mixing. Sensitive detection and separation of hydrolysed samples (amino acids) were achieved with the use of high-performance liquid chromatography (HPLC). The chromatographic column was preptreated with ophthalaldehyde, 3- mercaptopropionic acid (OPA/MPA), and 9- fluorenyl-methyl chloroformate (FMOC). The pre-column preparation was fully automated and had a detection range of 100-3000 pmoles, thus requiring only a small sample (1 µl). Three samples of isolated collagen fibers (ca. 5 µg each) from samples collected at different collection sites were analyzed using Waters PicoTag Work Station for gas phase Hydrolysis and Hewlett Packard 1090 HPLC equipped with a diode array detector and an auto injector with a PC based Chemstation database, utilizing Amino Quant chemistry.

2.5 Ultrastructure analyses

2.5.1 Scanning electron microscopy (SEM and E-SEM)

For scanning electron microscopy, samples from the polypary, ~ 3 cm^2 each, and isolated fibers were fixed in 4% glutaraldehyde in filtered seawater (0.22 µm FSW). These samples were dehydrated through a graded series of ethanol (up to 100%), and critical- point dried with liquid CO_2. The polypary preparations were fractured using the tips of fine forceps to expose the gastrovascular cavities. These samples were coated with gold for SEM evaluation (SEM Jeol-840a). In addition, fibers were dehydrated as described above, coated with a gold-palladium alloy for ESEM evaluation(ESEM, JSM-6700 Field Emission Scanning Electron Microscope). Measurements on fiber and fibril diameters was performed using the Image J program (Schneider et al., 2012).

2.5.2 Transmission electron microscopy (TEM)

Samples were fixed as described above and then decalcified, twice, in a mixture of equal volumes of 50% (v/v) formic acid and 15% (w/v) sodium citrate for 20 minutes, and then placed in 4% glutaraldehyde and dehydrated through a graded series of ethanol (Dykstra and Reuss, 2003). The samples were embedded in Epon and the sections were stained with both uranyl acetate and lead citrate. Glycoproteins were detected by using sodium tungstate and cupromeronic blue staining (Scott, 1990). Negative staining was employed to study fibrils that were detached from fibers by sonication at 30 KHz for five minutes (PCI 1.5) (Ortolani and Marchini, 1995). TEM was carried out on a Jeol 1200 EX electron microscope.

2.6 X-ray Fiber Diffraction Data

X-ray fiber diffraction on dry collagen fibers from *S. ehrenbergi* was performed at the Biophysics Collaborative Access Team (BioCAT, ID18) and the Biology Center for Advanced Radiation Sources (BioCARS, ID14), at the Advanced Photon Source, Argonne National Laboratory, Chicago IL (Barrea et al., 2014). Similar diffraction data from native, hydrated, rat tail tendon and lamprey notochord were obtained from previous studies (Orgel et al., 2006; Antipova and Orgel, 2010; Orgel et al., 2000) and from linked RCSB codes (3HR2 and / or 3HQV) . The scaled amplitudes of the central, meridional section of each data set were used to calculate electron density maps. These data for type II collagen were published as supplementary information to Antipova and Orgel, 2010 (Antipova and Orgel, 2010). Electron density maps were calculated according to the methods published previously (Antipova and Orgel, 2010).

2.6.1 Comparison between X-ray and TEM derived Electron densities

A one dimensional line profile was computed from TEM images of thin-fibrils across ~ 220 nm for an exceptionally well resolved fibril. The region corresponding to 2 D-periods (each D-period of ~ 67 nm) was recognizable. The average line profile for these D-periods were then compared with the analogous D-period line profile, aka a one dimensional electron density map, obtained from the combination of structure factors as explained in the results section.

3 Results

3.1 Histological evaluation of collagen fibers

To establish the localization and type of collagen (fibrillar or network forming) in the mesentery of *S. ehrenbergi*, Masson's Trichome stain was performed. A histological cross-section of the uppermost part of a polyp below the pharyngeal level reveals the free edge of the mesenteries which are directed towards the center of the gastrovascular cavity (Fig. 2A). The mesenterial filaments of six out of the eight mesenteries feature an inner part, which when stained by Masson's Trichrome, give a specific turquoise color. This is indicative of the presence of collagen. The fibers pulled out from the polypary of *S. ehrenbergi* exhibit bundles, each comprised of numerous fibers (Mandelberg et al., 2016; Sharabi et al., 2014). Isolated fibers (Fig. 1) stained with Masson's Trichrome resulted in the same turquoise color, indicative of collagen (Fig. 2B). The fibers are approximately 9 μm in diameter and they form bundles featuring a width of 100-200 μm, resembling coiled structures, as seen in TEM micrographs (see electron microscopy section below) (Mandelberg et al., 2016; Sella, 2012). This arrangement of fibers is used as a hydro skeleton to support the colonies biomechanically. In addition, these fibers also accommodate the extra load rendered by the gonads borne by the mesenteries. The coiled collagen fibers within the mesenteries have already been described for *S. auritum* (Mandelberg et al., 2016), but have not been described in any other cnidarian or invertebrate. It seems, therefore, that the new structure and arrangement of the fibers reported here are unique both in their location and structure in the soft coral colony and thus pose importance for the soft coral structure.

3.2 Protein and amino acid analysis

27 distinct peaks were recorded on the HPLC profile (Fig.3). 19 of these peaks were recognized and and quantified. The unidentified peaks might be a result of additional amino acids, which are common in marine organisms and are known as non-proteinogenic amino acids (NPAA) (Nelson et al., 2003). NPAA are typically formed as a result of post-translational modifications or as intermediates in metabolic processes (Curis et al., 2005). Hydroxyproline is a one such NPAA that is important for stabilizing the packing structure of fibrillar collagens, as it participates in the formation of enzymatic crosslinks (Orgel et al., 2000). Aeration of peptide bonds by sea water also results in the modification of amino acids in these organisms (McDowell et al., 1999).

High concentrations of glycine, proline and hydroxyproline, relative to non-collagenous proteins, identify with other fibrillar collagens with similar concentrations of these amino acids (Table 1). The overall similarity in the amino acid content from *S. ehrenbergi* in comparison to rat type I and human type II collagen allows for the interpretation that the molecular and fibrillar packing structure of collagen in these fibers is indeed similar. A comparison between the amino acid content of the *S. ehrenbergi* collagen presented here and other fibrillar and network forming collagens is discussed in supplementary information. (See Table S1).

3.3 Ultrastructural analysis using electron microscopy

The micrographs of fibrils in longitudinal sections exhibited a repeating pattern of dark and light banding perpendicular to the fiber axis and are reminiscent of the fibrillar collagen D-band repeat that were not homogeneously stained as typical to collagen. The diameter of the fibrils in the cross sections was 15.16 ±3.41 nm (n=17 fibrils in 6 fibers, Fig. 4D) and the width of thin fibers in the longitudinal sections was 15.9 ±3.11 nm (n=15 fibrils in 3 fibers, Fig. 4E).

An E-SEM analysis revealed that the fibrils are interwoven to form a three-dimensional arrangement, with free ends on some fibrils, and fused or bifurcated ends on others (Fig. 4F). Such an arrangement adds to the mechanical properties of the fibers and caters to the extent of tensile stress that octocorals experience in their natural environment. The presence of ends and bifurcations was evident in the fibers, displaying morphological features that are typical for growing fibers, as described in Mandelberg et al., 2016 (Mandelberg et al., 2016). Similar bifurcations and (fibril) fusions occur during the formation new collagen fibers in developing fetuses, in growth and in the regenerating scar tissues of mammals (e.g., rat (Provenzano and Vanderby Jr., 2006); sheep (White et al., 2002)). This would appear to be a feature shared between these octocoral collagen fibrils and fibers and the equivalent collagen fibrils and fibers of vertebrates. The average fibril and fibril-bundle (fiber) diameter measured from E-SEM images ranged from 14.48 to 38.93 nm, which correlates with the average diameter measured from TEM images (Fig.4D).

TEM images of fragments of negatively stained fibrils, isolated by sonication featured a diameter of 18.9 ±2.45 nm (n=41 measurements on 27 isolated fibrils, Figs 4 and 5) as well as a repeated, dark and light banding perpendicular to the fiber axis. Examination of this banding along the fibrils by creating a color intensity distribution showed dark and repeating bands every 65-70 nm (the D-periodic repeat), with some lower amplitude (less dark) repeating bands in the 65-70 nm zone (Figs 4 and 5), suggesting the pattern of mammalian fibrillar collagen. This D-period value is supported by the X-ray observations, see below. Furthermore, the negative staining of isolated fibrils revealed a parallel arrangement of thinner sub-structures ~ 3 nm wide (Fig. 5), protruding from the end of the fibril, which featured an uneven surface area (Fig. 5). This structure resembles that observed for type II collagen (Antipova and Orgel, 2010) where collagen microfibrils are observed at the fractured end of a collagen fibril. Microfibrils have been observed for type I and type II collagen and are believed to be a feature of fibrillar collagen in general, although for reasons of molecular architecture, are not separable from a type I fibril due to the cooperative nature of that fibrils construction. Whereas, independent microfibrils have been observed jutting from the end of a partially disrupted type II fibril.

From the TEM data, it was observed that there was an unstained area between adjacent thin-fibers. These fibers when stained with cupromeronic blue (CB), provide a strong dark blue coloring of proteoglycans (Fig. 4D). Fibers in the longitudinal sections of the CB stained samples, revealed a parallel arrangement of closely packed fibrils surrounded by a dense proteoglycan matrix (as determined from CB stain). This matrix seemed to be distributed evenly between the fibrils and along the fiber (Fig. 5D). When comparing the TEM micrographs of longitudinal sectioned fibers with CB stained fibers, (Fig. 4), it is evident that CB labeled the areas between adjacent fibrils within the fibers, structured in a manner found commonly in mammalian connective tissue fibrillar collagens.

3.4 X-ray diffraction and D-period electron density organization

X-ray diffraction, Fig. N, revealed a 66 nm meridional periodicity both in wet and dried preparations of octocoral collagen fibers, suggestive of an average molecular tilt of ~ 14° relative to fiber axis. This is in contrast to types I-III collagen that average about 10° from the fiber axis (with a 67 nm D-period) (Wess and Orgel, 2000). The meridional intensity distribution of the octocoral fibers differs from both type I or type II collagen which suggests that the D-period organization is non-identical (Fig. NB). The collagen helix layer lines are evident along the fiber axis (Fig. NB), and the pattern loosely resembles that of rat-tail tendon diffraction indicating a collagen triple helix (Fig.NA).

The similiarity in the amino acid content (Table 1) between the *S. ehrenbergi* collagen fibers and mammalian type I (rat) and type II (human) collagen, enables the systematic application of crystallographic information collected from the latter to x-ray diffraction and electron microscopy data reported herein. This process, known as molecular replacement, has been used over many decades to arrive at preliminary structures for new proteins (especially extracellular matrix proteins), that share similarities with proteins of know structure (Höhne, 1973; Tickle and Driessen, 1996). Furthermore, there is a stark similarity in the diffraction profile observed between *S. ehrenbergi* fibers and those of type I and II collagens as described in previous works (Antipova and Orgel, 2010, 2012; Orgel et al., 2006). Hence, it is prudent to calculate one dimensional electron density maps from the data in hand by combining structure factors and phase information from the previous structural determinations of types I and II collagen, with the amplitudes recorded from the octocoral diffraction patterns. This provides a means of estimating and observing the crystalline fibrillar D-periodic packing structure of the octocoral fibers. Fig N shows the 1D electron density profiles calculated using type I and II phases.

The electron density map generated with type I phases is scrambled, i.e. no gap-overlap step function and is significantly different from the original native type I map. Whereas there is an intelligible electron density map generated with the phases of vertebrate type II collagen in comparison with that generated from 'random' phases, or with those originating from the structure of type I collagen (Fig. N). This type II structure based electron density map shows a gap-overlap step function and resembles that of the native type II electron density map. This strongly indicates a fibrillar D-periodic organization of the octocoral fibers and suggests, that it may be closer to type II collagen structure than to type I. This alignment of electron density will not happen by pure chance, an estimate of which, conservatively, is in the order of 1 in 6 to the power of 13 assuming 60° error per phase and as is demonstrated by the selected electron density map formed from Octorcoral amplitudes but randomly generated phases.

An average electron density was calculated from the TEM of coral fibers over two D-periods (Fig. 8). Although it is tempting to point to the obvious similarities between the TEM and X-ray derived electron density maps, the fact that the TEM map was derived from only two D-periods (from an exceptionally clear section of TEM data), there should be great caution in assigning any value to their similarity, other than their gross overall similarity (for instance, the gap/overlap ratio). In this regard, the data obtained from the X-ray diffraction has much greater statistical significance (being derived from the X-ray contribution of millions of crystalline domains within the sample) over that of a TEM observation, even though these TEM observations confirm the X-ray data.

The X-ray diffraction derived electron density map is still sufficiently different to indicate that there are structural dissimilarities in packing organization, despite (1) its similarity to type II collagen; (2) the apparent organization (and fibril size) that resembles type II collagen; and (3) especially while the helical organization of the octocoral collagen resembles type I collagen (see Fig. N). These differences may be organizational or compositional or both. They could be due to amino acid content differences in the collagen protein itself and / or the deposition of highly organized ECM ligands such as proteoglycans on the surface of the fibrils / fibril-bundles.

4 Discussion

These cord-like collagen fibers exhibit a unique location and arrangement within the coral mesenteries, that are markedly differ from the mesoglea collagen. Their structural organization are unusual among cnidarian and here we demonstrate that they resemble vertebrate collagen in structural organization. It is possible that their intriguing differences in mechanical properties from that of mammalian collagens (Danto and Woo, 1993; Fung and Liu, 1995; Vogel, 2013) could well arise almost entirely from their proteoglycan rich organization, which might also be the underlying reason for their unique structure. In the mesoglea, fibrils are short and the matrix surrounding them is thick and soft (e.g. Metridium mesoglea). As a result, the mesoglea can withstand large strains (deform to several hundred percent extension) by the sliding of fibrils relative to their neighbors. Thus, it appears that the octocoral fibers are an extreme mesoglea component, which present tighter structural organization, more similar to that of a vertebrate tendon or ligament.

The difference in properties between the octocoral fibers and the vertebrate fibrillar collagens could be a result of the difference in the structure: of collagen fibrils, in the matrix between the fibrils, or the combination of both. Nevertheless, it is without doubt (to us) that based on our observations of molecular and structural organization, these coral fibers are much closer to tendon/ligament of vertebrate collagens than to the collagenous mesoglea typically seen in other cnidarians. These are unique fibers, and their role in the coral physiology is enigmatic. The similarity of D-periodic fibril structure between vertebrate type II collagen and this invertebrate form is striking, the major organizational differences perhaps coming from the very rich PG mediated organization. However, we cannot rule out the possibility of a unique collagen. Even if this be the case, its fibrillar D-periodic structure is clearly close to that of type II collagen of vertebrates, while the organization into fibril-bundles resembles that of type I collagen in tendons and ligaments of vertebrates. Regardless, the vast quantity of these organized bundles of fibers within *S. ehrenbergi* suggests that they do play a significant, yet still unknown role, in the octocoral physiology. Given that invertebrates account for at least 95% of animals, one can readily anticipate that they are a potential treasure trove of unique collagens.

Acknowledgments

Thanks the staff and scientists of the BioCAT group. Use of the Advanced Photon Source was supported by the U.S. Department of Energy, Basic Energy Sciences, Office of Science, under contract No. W-31-109-ENG-38. BioCAT is a National Institutes of Health-supported Research Center RR-08630. This research also used resources of the Advanced Photon Source, a U.S. Department of Energy (DOE) Office of Science User Facility operated for the DOE Office of Science by Argonne National Laboratory under Contract No. DE-AC02-06CH11357.

Competing interests

The authors declare no competing interests.

Funding

Use of BioCARS was also supported by the National Institute of General Medical Sciences of the National Institutes of Health under grant number R24GM111072. The content is solely the responsibility of the authors and does not necessarily reflect the official views of the National Institutes of Health. This work was also supported by the National Science Foundation (Grant #MCB-0644015 CAREER) and this material is based upon work supported by, or in part by, the U.S. Army Research Laboratory and the U.S. Army Research Office under contract/grant number W911NF-11-2-0018-P00002. Grant form the Israeli Ministry of Science number 00040047000 to DB. We would like to thank M. Weis for assistance in the field and laboratory work. We acknowledge the staff of the Interuniversity Institute for Marine Sciences in Eilat (IUI) for facilities. This research was in part supported by the Israel Cohen Chair in Environmental Zoology to YB. Collection animals complied with a permit issued by the Israel Nature and National Parks Protection Authority.

Author Contributions

YB, IS, YM performed sample collection. IS, YM, YK, DB performed fiber characterization and protein analysis studies. JPRO, OA, and IS (Antipova and Orgel, 2010; Orgel and Sella, 2012) performed x-ray diffraction experiments and data interpretation. YB, DB, IS, RM, JPRO, drafted the manuscript. All authors gave final approval for publication.

References

Antipova O. and Orgel J. P. R. O. . In situ D-periodic molecular structure of type II collagen. *The Journal of Biological Chemistry*, 285 (10): 7087–7096, Mar. 2010.

Antipova O. and Orgel J. P. R. O. . Non-Enzymatic Decomposition of Collagen Fibers by a Biglycan Antibody and a Plausible Mechanism for Rheumatoid Arthritis. *PLOS ONE*, 7 (3): e32241, Mar. 2012.

Barrea R. A. , Antipova O. , Gore D. , Heurich R. , Vukonich M. , Kujala N. G. , Irving T. C. , and Orgel J. P. R. O. . X-ray micro-diffraction studies on biological samples at the BioCAT Beamline 18-ID at the Advanced Photon Source. *Journal of Synchrotron Radiation*, 21 (5): 1200–1205, Sept. 2014.

Brazel D. , Oberbäumer I. , Dieringer H. , Babel W. , Glanville R. W. , Deutzmann R. , and Kühn K. . Completion of the amino acid sequence of the α1 chain of human basement membrane collagen (type iv) reveals 21 non-triplet interruptions located within the collagenous domain. *The FEBS Journal*, 168 (3): 529–536, 1987.

Bütikofer U. , Fuchs D. , Bosset J. O. , and Gmür W. . Automated HPLC-amino acid determination of protein hydrolysates by precolumn derivatization with OPA and FMOC and comparison with classical ion exchange chromatography. *Chromatographia*, 31 (9-10): 441–447, May 1991.

Curis E. , Nicolis I. , Moinard C. , Osowska S. , Zerrouk N. , Benazeth S. , and Cynober L. . Almost all about citrulline in mammals. *Amino Acids*, 29 (3): 177–205, Nov 2005.

Danto M. I. and Woo S. L.-Y. . The mechanical properties of skeletally mature rabbit anterior cruciate ligament and patellar tendon over a range of strain rates. *Journal of Orthopaedic Research*, 11 (1): 58–67, Jan. 1993.

Dykstra M. J. and Reuss L. E. . *Biological Electron Microscopy Theory, Techniques, and Troubleshooting*. Springer US, Boston, MA, 2003.

Exposito J.-Y. , Larroux C. , Cluzel C. , Valcourt U. , Lethias C. , and Degnan B. M. . Demosponge and sea anemone fibrillar collagen diversity reveals the early emergence of A/C clades and the maintenance of the modular structure of type V/XI collagens from sponge to human. *The Journal of Biological Chemistry*, 283 (42): 28226–28235, Oct. 2008.

Exposito J.-Y. , Valcourt U. , Cluzel C. , and Lethias C. . The Fibrillar Collagen Family. *International Journal of Molecular Sciences*, 11 (2): 407–426, Jan. 2010.

Fabricius K. and Alderslade P. . *Soft corals and sea fans: a comprehensive guide to the tropical shallow water genera of the central-west Pacific, the Indian Ocean and the Red Sea*. Australian Institute of Marine Science, Townsville, Qld, 2001.

Fautin D. G. and Mariscal R. N. . *Cnidaria: anthozoa*. Wiley-Liss, 1991.

Fung Y. C. and Liu S. Q. . Determination of the mechanical properties of the different layers of blood vessels in vivo. *Proceedings of the National Academy of Sciences*, 92 (6): 2169–2173, Mar. 1995.

Gathercole L. , Atkins E. , Goldbeck-Wood E. , and Barnard K. . Molecular bending and networks in a basement membrane-like collagen: packing in dogfish egg capsule collagen. *International journal of biological macromolecules*, 15 (2): 81–88, 1993.

Glanville R. W. . Type iv collagen. *Structure and function of collagen types*, pages 43–79, 1987.

Höhne E. . M. g. rossmann (editor). the molecular replacement method. a collection of papers on the use of non-crystallographic symmetry. gordon and breach, london 1972. international science review series nr. 13 (edited by lewis KLEIN) 33 beiträge, 267

seiten mit zahlreichen abbildungen. preis 6.25. *Kristall und Technik*, 8 (12): K51–K51, 1973.
Knupp C. and Squire J. . X–ray diffraction analysis of the 3d organization of collagen fibrils in the wall of the dogfish egg case. *Proceedings of the Royal Society of London B: Biological Sciences*, 265 (1411): 2177–2186, 1998.
Mandelberg Y. , Benayahu D. , and Benayahu Y. . Octocoral Sarcophyton auritum Verseveldt & Benayahu, 1978: Microanatomy and Presence of Collagen Fibers. *The Biological Bulletin*, 230 (1): 68–77, Feb. 2016.
McDowell L. M. , Burzio L. A. , Waite J. H. , and Schaefer J. . Rotational echo double resonance detection of cross-links formed in mussel byssus under high-flow stress. *Journal of Biological Chemistry*, 274 (29): 20293–20295, jul 1999.
Nelson D. L. , Cox M. M. , and Lehninger A. L. , editors. *Lehninger principles of biochemistry*. Worth Publ, New York, NY, 3. ed., 7., printing edition, 2003. OCLC: 249106180.
Orgel J. P. , Wess T. J. , and Miller A. . The in situ conformation and axial location of the intermolecular cross-linked non-helical telopeptides of type I collagen. *Structure*, 8 (2): 137–142, Feb. 2000.
Orgel J. P. R. O. , Irving T. C. , Miller A. , and Wess T. J. . Microfibrillar structure of type I collagen in situ. *Proceedings of the National Academy of Sciences*, 103 (24): 9001–9005, June 2006.
Ortolani F. and Marchini M. . Cartilage type II collagen fibrils show distinctive negative-staining band patterns differences between type II and type I unfixed or glutaraldehyde-fixed collagen fibrils. *Journal of Electron Microscopy*, 44 (5): 365–375, Oct. 1995.
Petruska J. A. and Hodge A. J. . A Subunit Model for the Tropocollagen Macromolecule. *Proceedings of the National Academy of Sciences*, 51 (5): 871–876, May 1964.
Provenzano P. P. and Vanderby Jr. R. . Collagen fibril morphology and organization: Implications for force transmission in ligament and tendon. *Matrix Biology*, 25 (2): 71–84, Mar. 2006.
Ross M. H. and Pawlina W. . *Histology: a text and atlas: with correlated cell and molecular biology*. Lippincott Wiliams & Wilkins, Baltimore, MD, 5th ed edition, 2006.
Schneider C. A. , Rasband W. S. , and Eliceiri K. W. . NIH Image to ImageJ: 25 years of image analysis. *Nature Methods*, 9 (7): 671–675, July 2012.
Schwarz U. , Schuppan D. , Oberbäumer I. , Glanville R. W. , Deutzmann R. , Timpl R. , and Kühn K. . Structure of mouse type iv collagen. *The FEBS Journal*, 157 (1): 49–56, 1986.
Scott J. E. . Proteoglycan:collagen interactions and subfibrillar structure in collagen fibrils. Implications in the development and ageing of connective tissues. *Journal of Anatomy*, 169: 23–35, Apr. 1990.
Sella I. . *Biological, biochemical, and mechanical properties of collagen fibers of the soft coral Sarcophyton ehrenbergi*. PhD thesis, Tel-Aviv University, Tel-Aviv, Israle, 2012.
Sharabi M. , Mandelberg Y. , Benayahu D. , Benayahu Y. , Azem A. , and Haj-Ali R. . A new class of bio-composite materials of unique collagen fibers. *Journal of the Mechanical Behavior of Biomedical Materials*, 36: 71–81, Aug. 2014.
Sharabi M. , Benayahu D. , Benayahu Y. , Isaacs J. , and Haj-Ali R. . Laminated collagen-fiber bio-composites for soft-tissue bio-mimetics. *Composites Science and Technology*, 117: 268 – 276, 2015.

Sharabi M. , Varssano D. , Eliasy R. , Benayahu Y. , Benayahu D. , and Haj-Ali R. . Mechanical flexure behavior of bio-inspired collagen-reinforced thin composites. *Composite Structures*, 153: 392 – 400, 2016.
Swatschek D. , Schatton W. , Müller W. , and Kreuter J. . Microparticles derived from marine sponge collagen (SCMPs): preparation, characterization and suitability for dermal delivery of all-trans retinol. *European Journal of Pharmaceutics and Biopharmaceutics: Official Journal of Arbeitsgemeinschaft Für Pharmazeutische Verfahrenstechnik e.V*, 54 (2): 125–133, Sept. 2002.
Tickle I. J. and Driessen H. P. C. . *Molecular Replacement Using Known Structural Information*, pages 173–203. Humana Press, Totowa, NJ, 1996.
Vogel S. . *Comparative biomechanics: life's physical world*. Princeton University Press, Princeton, second edition edition, 2013.
Wess T. J. and Orgel J. P. . Changes in collagen structure: drying, dehydrothermal treatment and relation to long term deterioration. *Thermochimica Acta*, 365 (1–2): 119–128, Dec. 2000.
White J. F. , Werkmeister J. A. , Darby I. A. , Bisucci T. , Birk D. E. , and Ramshaw J. A. M. . Collagen fibril formation in a wound healing model. *Journal of Structural Biology*, 137 (1-2): 23–30, Feb. 2002.

Figures

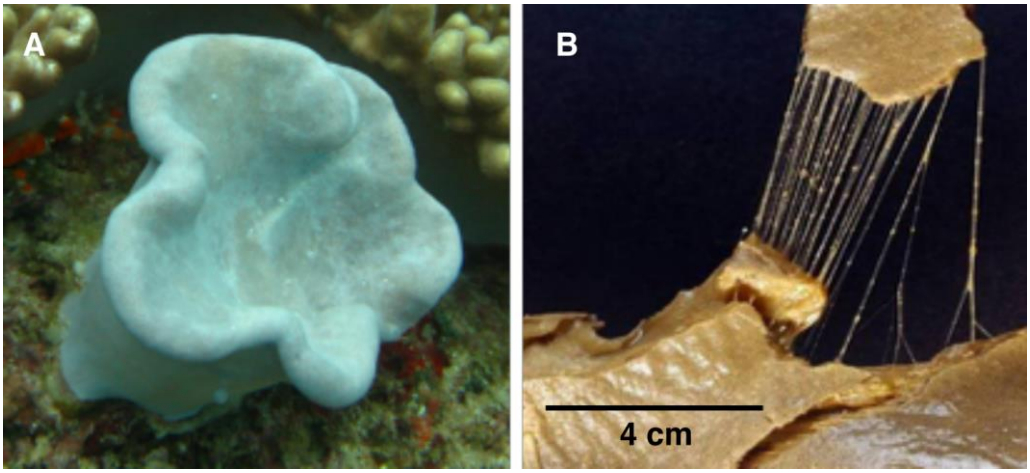

Figure 1: **A)** Underwater image of the octocoral *Sarcophyton ehrenbergi*, **B)** Torn apart colony revealing collagen fibers.

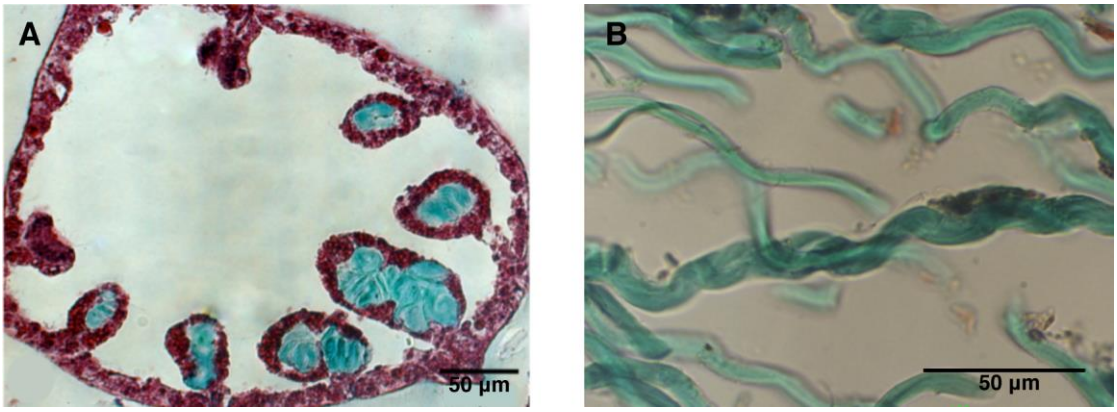

Figure 2: **A)** Masson's Trichrome stained histological cross-section of uppermost part of a polyp below pharyngeal level reveals free edge of mesenteries loaded with turquoise stained collagen fibers directed towards the center of the gastrovascular cavity, light-stained periphery indicating the non-fibrous collagen, **B)** Isolated fibers stained with Masson's Trichrome resulted in turquoise color indicative of collagen.

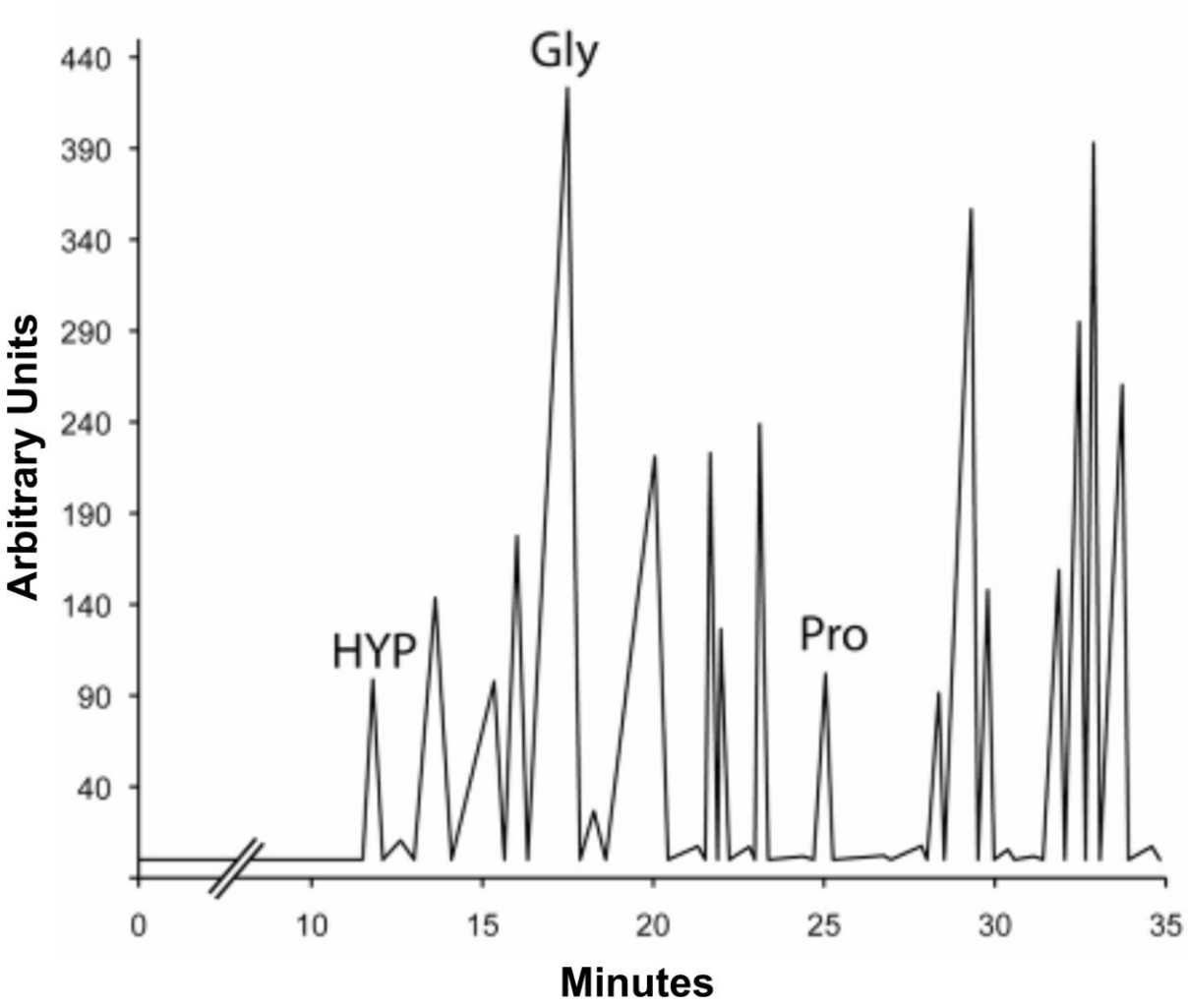

Figure 3: **HPLC profile from hydrolysate of fibers.** This profile was analyzed using the Chemstation Database and the Glycine (Gly), Proline(Pro) and Hydroxyproline (HYP) are marked respectively.

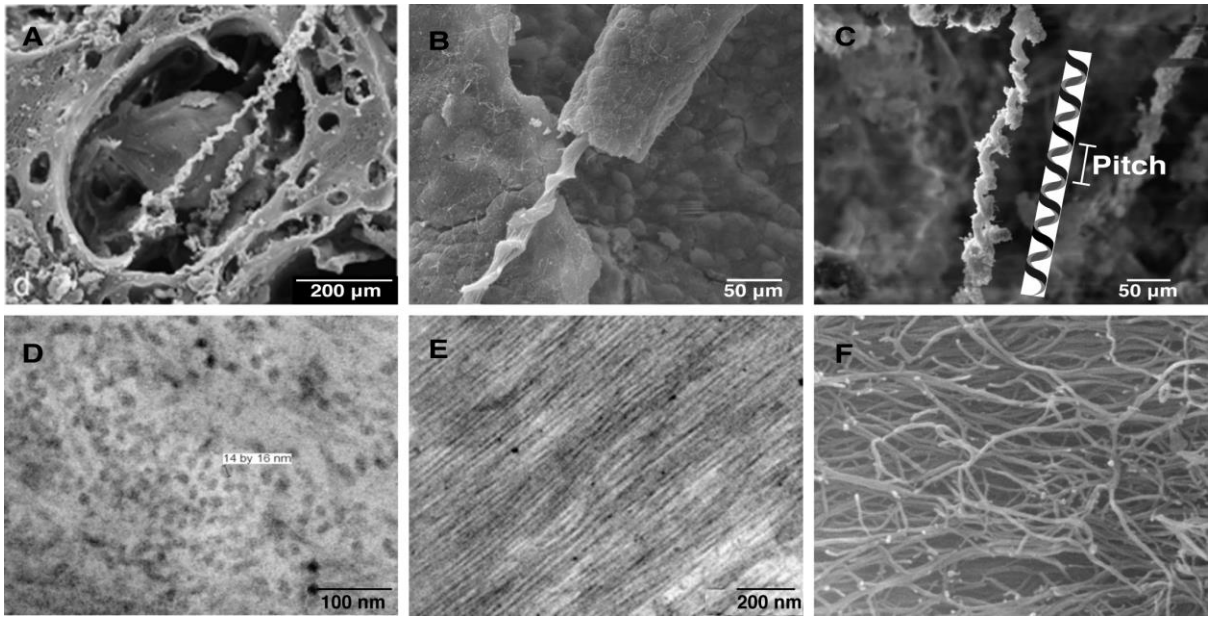

Figure 4: **Electron microscopy on collagen fibers from the *S. ehrenbergi*. A,B,C:** SEM Images of fibers emerging from an exposed polyp cavity, the helical structure and the fibrillar texture of the fibers (insert) are noted; TEM Image of **D:** Cross-section and **E:** Longitudinal section of a fiber; **F:** E-SEM Image of isolated collagen fibers showing fibrils exhibiting interweaving configuration with fibril ends and fiber bifurcations.

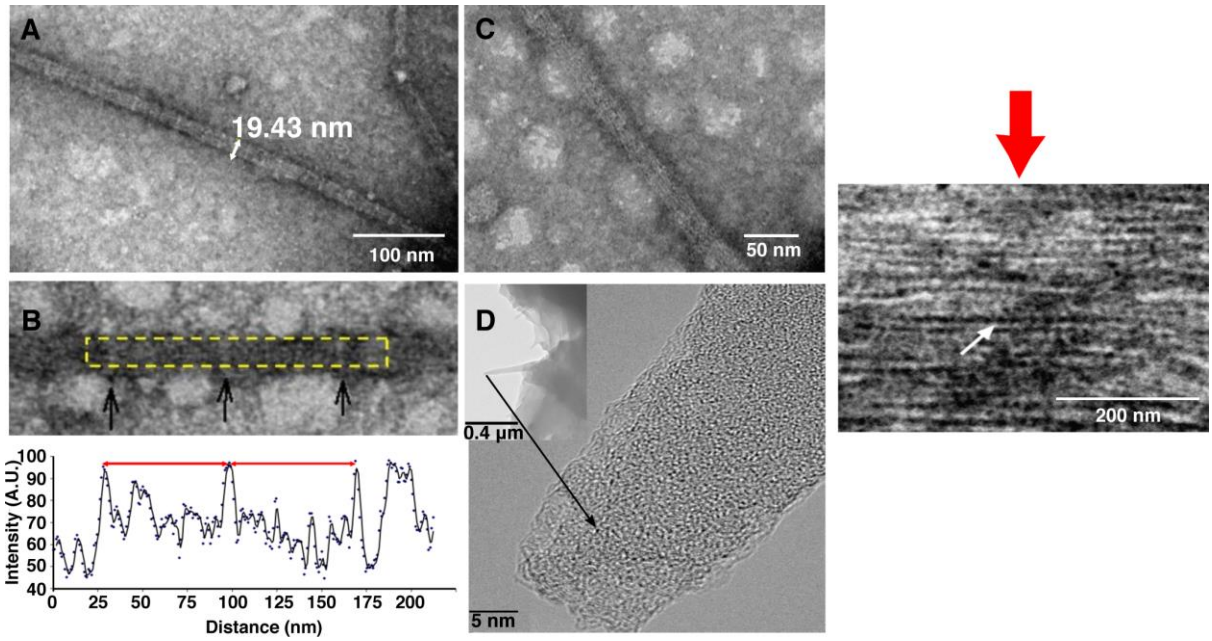

Figure 5: **A)** TEM micrograph of isolated positively stained fiber of octocoral *Sarcophyton ehrenbergi*, showing organized D-period substructure. **B)** One dimensional scan of two D-periods (as shown) which assigns relative 'intensity' to the relative electron density of each part of the D-period which is approximately 66 nm in length **C)** Negatively stained fiber, shows composition from still thinner fibers, thin-fibrils. **D)** 'ground substance' between collagen fibers, likely composed of GAG rich proteoglycans.

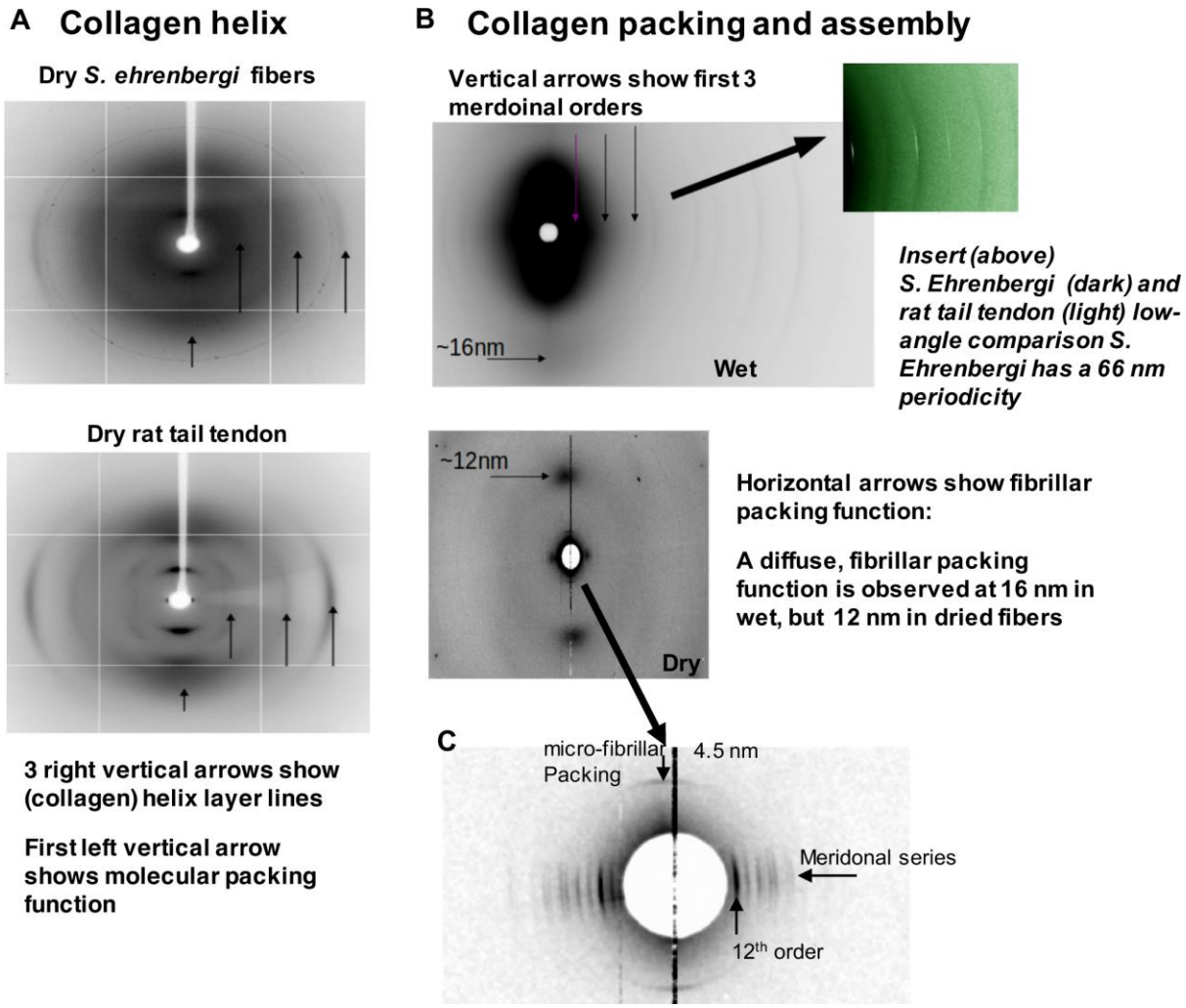

Figure 6: **X-ray diffraction patterns. A)** Wide angle X-ray diffraction of dry *Sarcophyton ehrenbergi*, fibers and dry rat tail tendon, the helix layer lines / meridional reflections originating from the molecular transform (16), appear to similar. **B)** Low angle, wet and dry coral fiber-diffraction. Note fibril interference function between 12-16nm. In the fiber diffraction of the wet fibers, the meridional diffraction originating from the D-period is evident, as per that seen in rat-tail tendon. The first 3 orders of this diffraction series (as do 3-8 shown in the insert) conform to a periodicity of 66 nm, which is directly analogous to the 67 nm D-periodicity of rat tail tendon. INSERT: X-ray diffraction low-angle (meridional orders 3-8) comparison of *Sarchophyton ehrenbergi* (dark) with 66 nm periodicity super imposed on rat tail tendon (light) with its 67 nm periodicity. **C)** Medium angle fiber diffraction of coral fibers. Note the packing function at 4.5 nm, which is the same value seen for the collagen type I and II microfibril (Antipova and Orgel, 2012; Orgel et al., 2006).

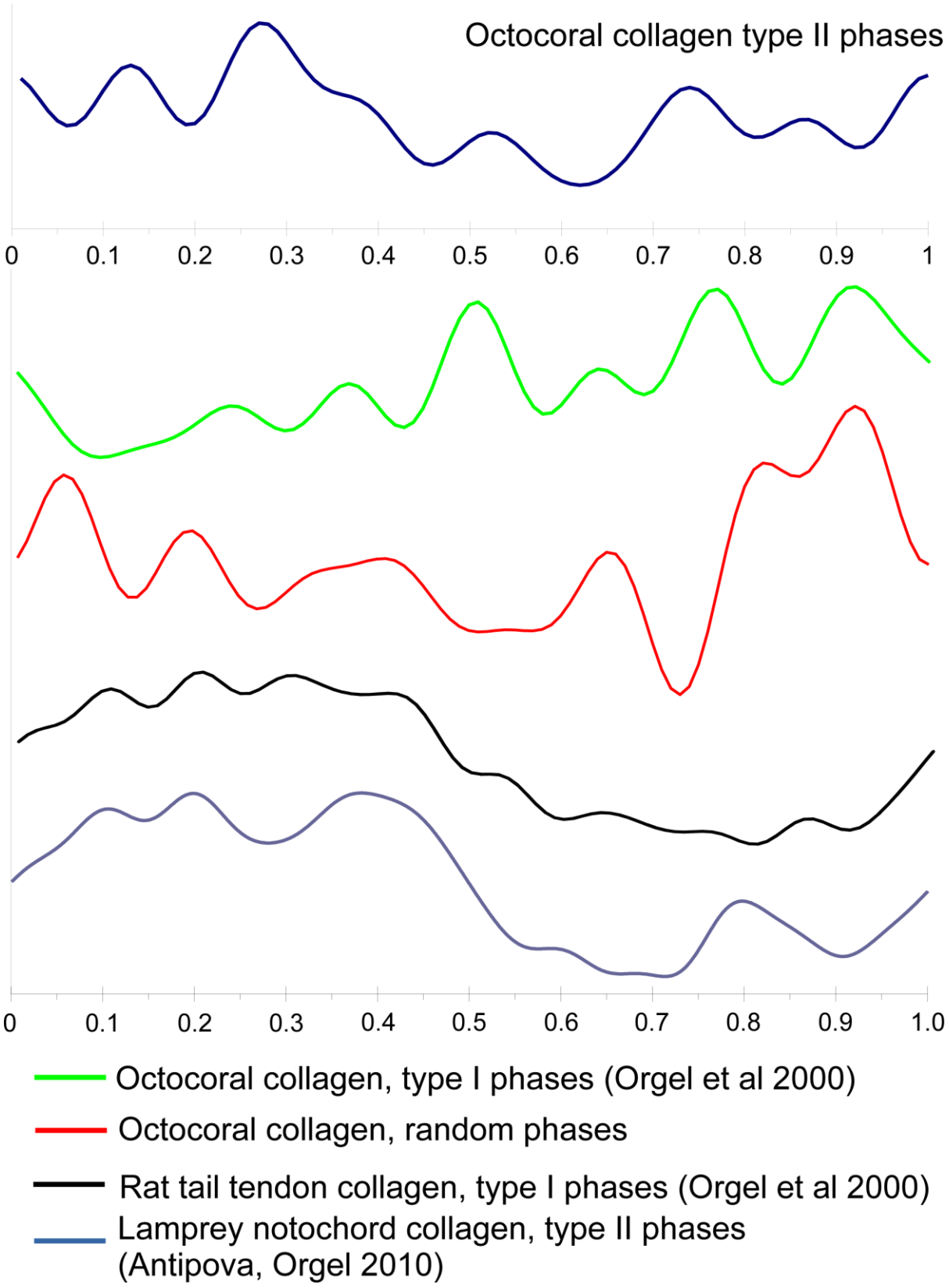

Figure 7: **X-ray derived electron density maps.** Extracted amplitudes from the low-angle meridional diffraction pattern of hydrated fibers of *S. ehrenbergi* combined with the phase information from different sources based on the principle utilized by molecular replacement. Here, the phases of type I and type II collagen (rat tail tendon and lamprey notochord) were each combined with the meridional derived amplitudes of the octocoral. A random set of phases was also applied in the same manner for comparison with the Fourier maps

generated from the use of the type I and type II collagen phases. The original 1D Fourier maps of type I and type II collagen using their respective amplitude and phase sets as per their original publications are also shown for comparison (see color key). This shows that of the three 'phase replacement' Fourier maps (type I, type II and random phases), the only intelligible one-dimensional Fourier map calculated from the octocoral amplitudes and that resembles a fibrillar collagen map, is the one with the collagen type II phases (blue). The presence of a gap-overlap in the coral electron density map while not identical to either the native type I or type II collagen map (black and light blue, bottom) in its D-period organization, it does shows enough similarity to imply a common organization in the D-period substructure.

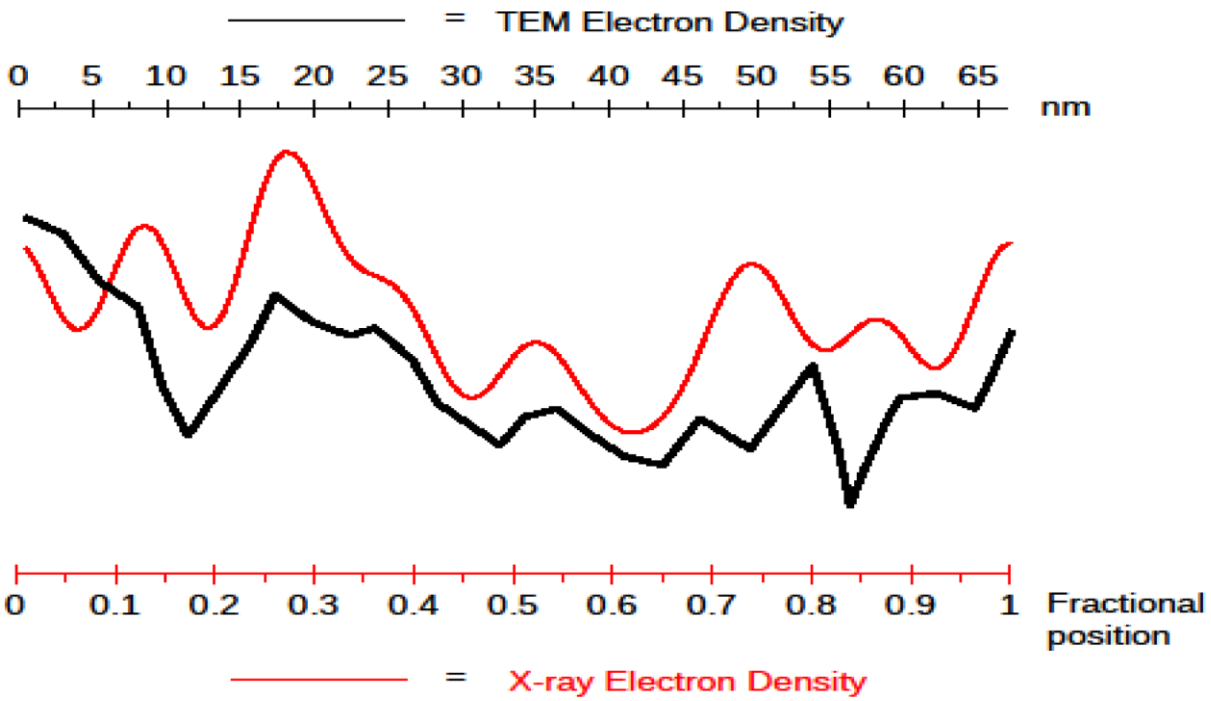

Figure 8: **Comparison of electron densities of the D-period sub-structure of *Sarcophton ehrenbergi* fibrils determined from TEM and X-ray diffraction.**

Table 1: Comparison of amino acid content between *S. ehrenbergi*, type I collagen from rat tail tendon (RTT) and Human type II collagen.

	Amino acid content (%)		
	S. ehrenbergi	RTT Type I collagen	Human type II collagen
Hpro	4.15	9.96	NA
Asp	8.34	1.53	1.67
Ser	4.35	4.18	3.27
Glu	9.52	4.56	5.18
Gly	24.89	33.22	31.87
His	0.94	0.41	0.56
Arg	5.35	4.95	5.02
Thr	3.43	2.04	2.31
Ala	6.49	10.53	9.96
Pro	5.08	12.00	21.27
Tyr	1.52	0.35	0.64
Val	3.97	2.36	1.43
Met	1.96	0.67	0.56
Lys	2.96	2.97	3.67
Ile	2.47	1.12	1.59
Leu	3.29	2.39	2.63
Phe	1.69	1.21	1.04

Molecular and Ultrastructural Studies of a Fibrillar Collagen from Octocoral (Cnidaria)

Orgel et al.

June 30, 2017

Supplementary information

Amino acid sequences of fibrillar and non-fibrillar collagens

Over 25 types of fibrillar and non-fibrillar collagens have been reported in humans. However, only fibrillar (ex. type I and II) and network forming (type IV) types of collagen have been reported in the earliest branches of multicellular organisms such as Cnidarians (Exposito et al., 2008). The amino acid composition of type IV collagen from humans has been under evaluation for decades. The usual G-X-Y repeat found in fibrillar collagens is often found to be disrupted in human type IV collagen (Glanville, 1987). There are considerable differences in macromolecular structure of these two collagen types. These differences are a result of the amino acid composition and positioning of the X and Y amino acids within the G-X-Y repeat itself, between the two types of collagen (Ulla et al., 1986, Brazel et al., 1987). As demonstrated in the table, there is a higher concentration of glycine in the *S. ehrenbergi* collagen than in non-fibrillar collagen (type IV), further validating that the former is a fibrillar form of collagen.

Table S1 expands on the amino acid differences presented in Table 1. The differences in the amino acid composition between the various types of collagen lends further validates the interpretations made on the structure of the fibrillar collagen described here.

Table S1: Comparison of amino acid contents between type I (fibrillar) and type IV (network forming) collagens from *S. ehrenbergi* with other species. The accession numbers of the sequences are indicated respectively.

	S. ehrenbergi	Rat Type I Collagen	Human-Type II,Collagen	Human- Col4α1	Cnidarian- Col 4α1*
		(3HR2_A, 3HR2_B)	(P02458)	(AAI51221)	(KXJ15387)
G	24.89	33.22	31.87	28.64	17.80
P	5.08	12.00	21.27	19.47	12.20
Hyp†	4.15	9.96	0.00	0.00	0.00
A	6.49	10.53	9.96	3.48	4.27
R	5.35	4.95	5.02	2.70	5.00
E	9.52	4.56	5.18	4.19	3.54
S	4.35	4.18	3.27	4.31	6.71
D	8.34	2.84	3.27	3.48	4.88
K	2.96	2.97	3.67	5.57	7.56
Q	n/a	2.71	2.95	4.31	2.93
T	n/a	2.04	2.31	2.58	4.88
L	3.29	2.39	2.63	5.51	6.22
V	3.97	2.36	1.43	3.06	5.12
F	1.69	1.21	1.04	2.76	1.83
N	n/a	1.53	1.67	0.96	3.29
M	1.96	0.67	0.56	1.86	2.56
I	2.47	1.12	1.59	3.48	4.76
Y	1.52	0.35	0.64	1.08	2.44
H	n/a	0.41	0.56	1.02	1.34
C	n/a	0.00	0.64	1.20	1.46
W	n/a	0.00	0.48	0.36	1.22

*Partial sequence available.

† Hyp = Hydroxyproline.

Structural comparison of fibrillar and network forming collagens

Evident differences can be seen in the X-ray diffraction (XRD) patterns obtained from type IV collagen extracted from the wall of dogfish egg case when compared to those from fibrillar collagens, such as type I and II and the mesenterial collagen from *S. ehrenbergi*. A detailed XRD analysis on type IV collagen can be found in Gathercole et al., 1993 and Knupp and Squire, 1998. Electron microscopy and XRD information from these publications indicates a marked difference between these datasets from type IV and fibrillar (type I and II) collagen. For instance, TEM images from type IV collagen from the dogfish egg shell show an alternating banding pattern every 32 nm (Knupp and Squire, 1988). This banding pattern is considerably different form fibrillar collagens, in that there are more discreet striations within the D-perioidic repeat (67 nm) in fibrillar collagens.

Similar differences in XRD patterns can be observed. For example, the XRD patterns type IV collagen show a principle repeat of 81.2 nm (Knupp and Squire, 1998), whereas those from the collagen fibers from *S. ehrenbergi* show a principle repeat of 66 nm. This further validates the use of phase information from mammalian fibrilar collagen (type I and II) to derive 1-D electron density maps for the collagen fibers from *S. ehrenbergi*.